DOI: 10.1002/ejoc.200700966

Structural Elucidation with NMR Spectroscopy: Practical Strategies for Organic Chemists

Eugene E. Kwan*[a] and Shaw G. Huang[a]

Keywords: NMR spectroscopy / Configuration determination / Structure elucidation.

Practical strategies for the structural elucidation of small organic molecules are described for typical organic chemists. The analysis of an unknown is divided into three stages. First, structural connectivity is deduced from through-bond correlation experiments. Next, the relative stereochemistry is determined from NOE correlations and coupling constants (both proton–proton and proton–carbon). Finally, the proposed structure is verified by a careful inspection of all of the observed data. Tactics for the management of overlapping peaks, low sample concentrations, and high molecular weights are also described. This approach is illustrated by the step-by-step analyses of a simple test compound, menthol, and a complex polycyclic natural product, salvinorin A. Detailed procedures and sample data for menthol are provided as a practical tutorial. This will enable organic chemists to elucidate a wide range of complex structures by using modern NMR spectroscopic experiments.

1. Introduction

Since the early 1960s, NMR spectroscopy has become an indispensable tool for the characterization of organic molecules. Although early spectrometers were relatively insensitive and performed simple experiments at low-field strengths, they gave reliable measurements of chemical shifts and coupling constants. Later, spectrometers were much more sensitive and attained much higher field strengths, enabling the use of powerful 2D NMR experiments. In particular, the pairing of COSY (correlation spectroscopy) with directly detected heteronuclear correlation experiments (which link carbon atoms and nearby protons) proved particularly efficacious for determining structural connectivity.

When inverse detected heteronuclear correlation techniques (much more sensitive than their directly detected counterparts) were developed in the 1980s,[1] NMR became a practical alternative to X-ray crystallography for the elucidation of natural products. For example, these methods soon allowed the assignment of kauradienoic acid,[2] a complex diterpene, and even vitamin B_{12}.[3]

[a] Department of Chemistry and Chemical Biology, Harvard University,
12 Oxford Street, Cambridge, MA 02138, USA
Fax: +1-617-495-1460
E-mail: ekwan@fas.harvard.edu

Supporting information for this article is available on the WWW under http://www.eurjoc.org/ or from the author.

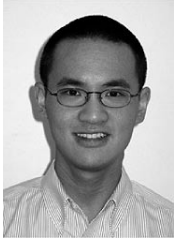

Eugene E. Kwan was born in Toronto in 1982. He completed his undergraduate degree in chemistry at the University of Toronto in 2004. His research there involved the synthesis of cyclopropane derivatives and the structural elucidation of natural products under the direction of Professor Robert A. Batey and Professor William F. Reynolds, respectively. Currently, he is undertaking PhD studies at Harvard University under the direction of Professor David A. Evans. He is presently engaged in a systematic investigation of diastereoselective intramolecular Michael reactions and their potential application in total synthesis.

Shaw G. Huang was born in Taiwan in 1949. He studied chemistry at the National University of Taiwan and later at Michigan State University, where he received his PhD under the supervision of Professor Max T. Rogers in the field of NMR theories and instrumentation. From 1977 to 1978, he worked as a research associate in the lab of Professor Jiri Jonas at the University of Illinois at Urbana-Champaign. In 1978, he was appointed the Director of NMR Laboratories in the Chemistry Department at Cornell University. In 1982, he moved to Harvard University where he remains as the Director of Magnetic Resonance Laboratories. His research interests are related to the development of NMR methodologies for the structural and dynamical studies of molecules.

Today, all but the most complex organic molecules are amenable to routine analysis, even with submilligram sample quantities. Recent work has uncovered the structural details of not only natural products of every class but also synthetic creations. Well-characterized examples include platensimycin (**1**),[4] a broad spectrum nonmevalonate terpenoid antibiotic, maoecrystal V (**2**),[5] an antitumor diterpenoid, chlorofusin, a peptide-based fungal metabolite with anticancer properties,[6] daphlongeranine B (**3**),[7] an unusual polycyclic alkaloid, and cytosporic acid (**4**),[8] a polyketide-derived HIV-1 integrase inhibitor, as well as β,β′-disilyl-substituted vinyl cations **5**[9] and cyanoresorc[5]arene **6**.[10]

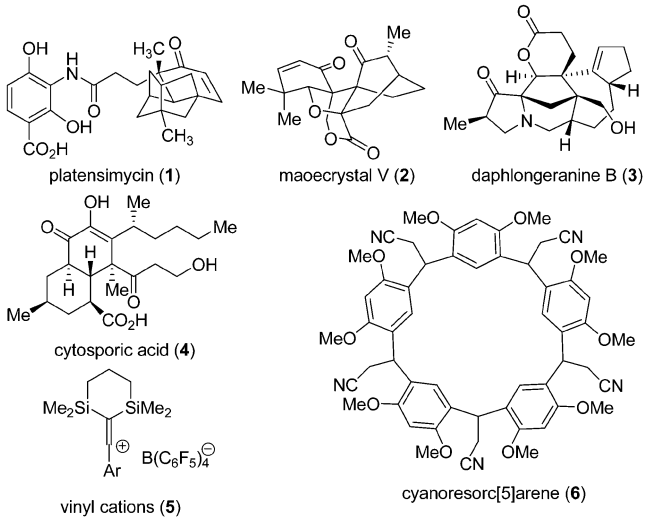

For simple unknowns, straightforward experiments such as 1D ^{1}H and ^{13}C NMR, COSY (correlation spectroscopy), and NOESY (nuclear Overhauser spectroscopy) suffice.[11] However, the spectra of complex molecules often contain overlapping peaks or higher-order multiplet patterns, which complicates interpretation.[12] Additionally, good-quality 1D ^{13}C NMR spectra can be challenging to obtain in a reasonable amount of time with small sample quantities, whereas compounds with high molecular weights (>750 Da) often give NOE correlations of weak intensity.[13] In such cases, an expanded approach that takes advantage of more powerful techniques is required.

Whereas the relative merits of many NMR pulse sequences have been described,[14] the practical details of how they can be combined to deduce organic structures have received less attention. This Microreview divides the process of structural elucidation into three phases: determination of skeletal connectivity, determination of relative stereochemistry, and verification of the proposed structure. Although many more techniques and experiments are undoubtedly more powerful than the ones described below, the following discussions are limited to techniques that have proven to be simple, versatile, reliable, and sensitive enough for routine use by nonexperts.

First, skeletal connectivity is deduced by combining data from both homonuclear (COSY) and heteronuclear (HSQC and HMBC) correlation spectroscopy. These experiments give good results even when significant overlap exists in the 1D ^{1}H NMR spectrum and do not require the time-consuming acquisition of a 1D ^{13}C NMR spectrum. Small structural fragments inferred from these data can, in turn, be iteratively combined to establish the overall connectivity of the unknown. Next, relative stereochemistry is inferred not only from NOE correlations between protons and proton–proton coupling constants ($^{n}J_{H,H}$), but also proton–carbon coupling constants ($^{n}J_{C,H}$). NOE-type correlations can now be effectively obtained for a broad range of molecular weights by using newer experiments, whereas many techniques are now available for extracting values of $^{n}J_{H,H}$ even when multiplet structures are obscured by spectral overlap. Measurements of $^{n}J_{C,H}$, now routinely available, provide an alternative line of evidence with which to support a proposed structure and can be obtained by using newer experiments. Finally, the proposed structure is verified in light of all of the observed data.

The following illustrates this approach by describing the step-by-step analyses of a simple test compound, menthol, and a complex natural product, salvinorin A (detailed experimental procedures and sample spectroscopic data are provided in the Supporting Information). Recommendations of acquisition and processing parameters for commonly used NMR spectroscopic experiments are given (Table 1), along with tactics for the management of large amounts of NMR spectroscopic data, overlapping peaks, low sample concentrations, and high molecular weights. Collectively, we hope this will serve as a valuable reference for organic chemists faced with complex structural elucidation tasks.

2. Determining Skeletal Connectivity

2.1. Initial Analysis

A cursory inspection of a one-scan 1D ^{1}H NMR spectrum should reveal most of the spectral features.[15] Although good quality spectra can be obtained even with low sample concentrations (<5 mM), high concentrations (>100 mM) can introduce artifacts and should be avoided. For example, a one-scan 1D ^{1}H NMR spectrum of menthol (Figure 1) shows a typical and perfectly acceptable result for a dilute solution. This is required because many 2D NMR spectroscopic experiments require the observation of ^{13}C satellites (relative intensity, 1). If even the parent ^{12}C peaks (relative intensity, 200) are not visible, further analysis may require excessive spectrometer time. In addition, compounds that exhibit complex or broad spectra due to impurities or tautomeric equilibria are typically not suitable for analysis.

It is prudent to obtain the molecular formula of the unknown by elemental analysis, or preferably, high-resolution mass spectrometry before any detailed analysis. The 1D ^{1}H NMR spectrum should be inspected to verify that the number of protons, as obtained by integration, matches the expected number from the molecular formula. This also al-

Table 1. Recommended acquisition and processing parameters.

Name[a]	Comments	Situation[b]	Acquisition Parameters[c]	Calibrations[d]	Processing Parameters[e]
COSY-45 (very high)	- off-diagonal peaks indicate coupled protons - gradient-selected	short survey	at=0.3, d1=0.8, ni=128, 10 min	90° (^{1}H) tune (^{1}H)	absolute-value; 2x LP in F1; sine-bell squared
		typical/dilute	at=0.3, d1=0.8, ni=256, 30 min higher resolution: ni=512, 1 h		
HSQC (high)	- peaks are protons directly attached to carbons - phases indicate whether CH_2 or CH/CH_3 - avoid sample heating: d1 > 4at ($CDCl_3$, CD_3OD) d1 > 10at ([D_6]DMSO) - probe tuning is essential	short survey	gradient-selected, at=0.1, d1=0.5, ni=32, j1xh=140, 30 min	90° (**^{1}H**, ^{13}C) tune (**^{1}H**, ^{13}C)	phase sensitive; 2x LP in F1; Gaussian
		typical	<500 Da: gradient-selected, at=0.2, d1=0.9, ni=128, j1xh=140, 2 h; >500 Da: gradient-selected, at=0.1, d1=0.5, ni=128, j1xh=140, 4 h		phase sensitive; 4x LP in F1; Gaussian
		dilute	- as above; use phase-cycled mode - turn spin-echo off (all peaks will have the same phase)	90° (**^{1}H**, **^{13}C**) tune (**^{1}H**, **^{13}C**)	
HMBC (low)	- peaks are protons within three bonds of carbon - one-bond doublets are common artifacts (J=$^{1}J_{C,H}$)	short survey	- use gradient-selected mode at=0.1, d1=0.5, ni=32, j1xh=140, jnxh=8, 30 min	90° (**^{1}H**, ^{13}C) tune (**^{1}H**, ^{13}C)	absolute value; 2x LP in F1; Gaussian
		typical	- use gradient-selected mode <500 Da: at=0.2,d1=0.9, ni=256, j1xh=140, jnxh=8, 4 h >500 Da: at=0.1, d1=0.5, ni=256, j1xh=140, jnxh=8, 8h		absolute value; 4x LP in F1; sine-bell (F1 and F2)
		dilute	- use phase-cycled mode	90° (**^{1}H**, **^{13}C**) tune (**^{1}H**, **^{13}C**)	F1 (phase), F2 (absolute); 4x LP in F1; Gaussian
1D DPFGSE NOESY/ tROESY (high)	- off-diagonal peaks are protons close in space - irradiated signal/ diagonal have opposite phase	short survey	0-750 Da: 1D NOESY, at=2.0, d1=1.0, mix=0.5, 64 scans, 5 min 750-2000 Da: 1D ROESY, at=1.0, d1=1.0, mix=0.4, 64 scans, 5 min	90° (^{1}H) tune (^{1}H)	standard 1D processing
2D NOESY/ tROESY (moderate)	- artifacts: COSY (alternating phase), exchange (OH, NH) (inverted)	typical	- use gradient-selected mode 200-750 Da: 2D NOESY, at=0.2, d1=1.3, ni=128, mix=0.6, 3 h 750-2000 Da: 2D ROESY: at=0.2, d1=0.8, ni=256, mix=0.4, 10 h	90° (**^{1}H**) tune (^{1}H)	phase sensitive; 4x LP in F1; Gaussian
1D TOCSY (very high)	- gives 1D ^{1}H subspectra for isolated spin systems	short survey	at=2.0, d1=2.0, mix=0.01 to 0.08 s, 64 scans, 5 min	90° (^{1}H) tune (^{1}H)	-standard 1D processing -use absolute value mode for significant phase distortions
		finding $^{n}J_{C,H}$	as above; at least 128 scans		

[a] Experiment (relative sensitivity). [b] Typical: 25 mM. Dilute: 1–5 mM. [c] Abbreviations: at (acquisition time, s), d1 (delay between scans, s), ni (number of increments), j1xh (estimated $^{1}J_{C,H}$, Hz), jnxh (estimated $^{n>1}J_{C,H}$, Hz), mix (mixing time, s). [d] Bold operations required; others recommended. [e] LP = linear prediction.

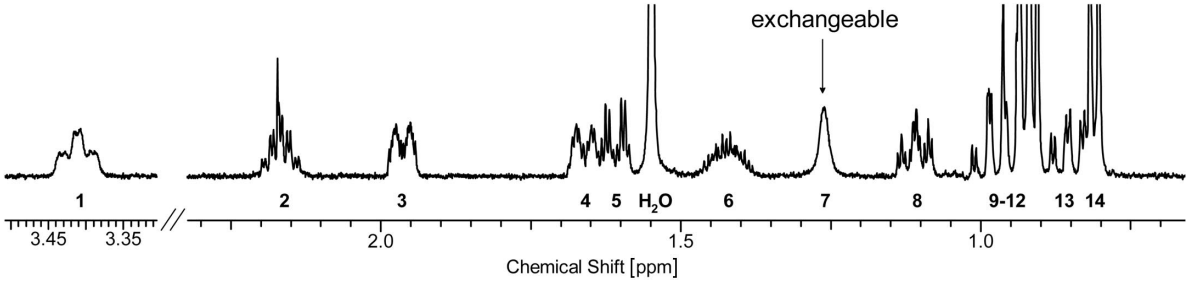

Figure 1. A dilute one-scan 1D ^{1}H NMR spectrum of menthol. Bold numbers identify each proton. (500 MHz, 0.5 mg in 700 μL $CDCl_3$ = 5 mM).

lows the "degree of unsaturation," U, or "index of hydrogen deficiency" to be calculated:[16]

$$U = C + 1 - \tfrac{1}{2}(H + X - N) \quad (1)$$

where C is the number of carbon atoms, H is the number of hydrogen atoms, X is the number of heteroatoms with valence 1 (e.g., halides), and N is the number of heteroatoms with valence 3 (e.g., nitrogen). U is the sum of the number of rings and multiple bonds present in the molecule and gives a useful starting point for analysis. Further information can be obtained from IR or UV/Vis spectra. The methods can quickly identify some functional groups; for example, many heterocycles have distinctive UV/Vis absorptions. For unknowns whose 1D ^{13}C NMR spectrum is avail-

able, reference to empirical tables of chemical shifts or computer predictions can give a wealth of information about what functional groups are present.[11]

2.2. One-Bond Heteronuclear Correlation (HSQC)

The next step is to identify each proton uniquely by using the HSQC (heteronuclear single quantum coherence) experiment.[17] The position of each peak in this phase-sensitive 2D experiment (one proton and one carbon axis) represents the chemical shift of every proton and its directly attached carbon. The major advantage of this procedure is that overlapping multiplets often become clearly separated peaks with identifiable chemical shifts. This works because resonances previously confined to one dimension (proton) become spread out over two dimensions (proton, carbon). For example, the HSQC spectrum of menthol shows thirteen unique correlations, clearly identifying the six closely spaced protons H(9)–H(14) (Figure 2).

In addition, the phase of each peak (typically represented with color) indicates whether its corresponding carbon atom is bonded to an even or odd number of protons.[18] Usually, this eliminates the need for edited 1D ^{13}C NMR experiments such as APT[19] or DEPT.[20] Thus, diastereotopic protons corresponding to methylene pairs can be readily identified, allowing geminal (two-bond) and vicinal (three-bond) COSY cross peaks to be distinguished. For example, in menthol, such methylene pairs are clearly CH_2(3,10), CH_2(4,13), and CH_2(5,9). Nondiastereotopic methylene pairs typically appear with roughly twice the intensity of nearby peaks.

Under typical conditions [hereafter defined as the use of a 5 mm inverse-detection probe with a 25 mM solution, which corresponds to 2.7 mg of compound (MW = 500) dissolved in 700 μL of solvent], this experiment requires approximately 1 h. Fair quality survey spectra can be obtained under the same conditions after only 15 to 30 min. This high sensitivity is possible because the experiment is proton-, rather than carbon-, detected ("inverse detection").

In general, HSQC spectra are very simple to interpret and free of artifacts. HSQC is substantially superior to the more common alternatives HMQC[21] and HETCOR[22] in terms of sensitivity, resolution, and spectral quality. By default, HSQC is optimized for a typical value of $^1J_{C,H}$ = 140 Hz. Protons with unusually high *s* character (e.g., terminal alkyne protons: $^1J_{C,H}$ = 250 Hz) may be attenuated or absent. Similarly, methyl protons arising from silyl protecting groups (e.g., *tert*-butyldimethylsilyl: $^1J_{C,H}$ = 120 Hz) are often missing.[23] Fortunately, the estimated value of $^1J_{C,H}$ can be tailored to the compound being analyzed (although this is rarely required). Appropriate experimental parameters for the HSQC and other experiments for a range of situations are given in Table 1.[24]

2.3. Working with NMR Spectroscopic Data

A convenient and effective method for working with large amounts of NMR spectroscopic data is demonstrated in Table 2 for menthol. For unambiguous identification, each unique group of protons is assigned a numerical label (ID) by using the HSQC spectrum (by convention, in ascending order from downfield to upfield). Proton and carbon chemical shifts are found from the center of 1D (when resolved or available) or HSQC peaks and are reported to two decimal places. Where resonances are very closely spaced but distinguishable, care is taken to label them consistently by using higher precision for chemical shifts if necessary. The chemical shifts of quaternary carbon atoms[18] can be obtained from 1D ^{13}C NMR spectra (if available) or HMBC/CIGAR correlations (see below). The number of

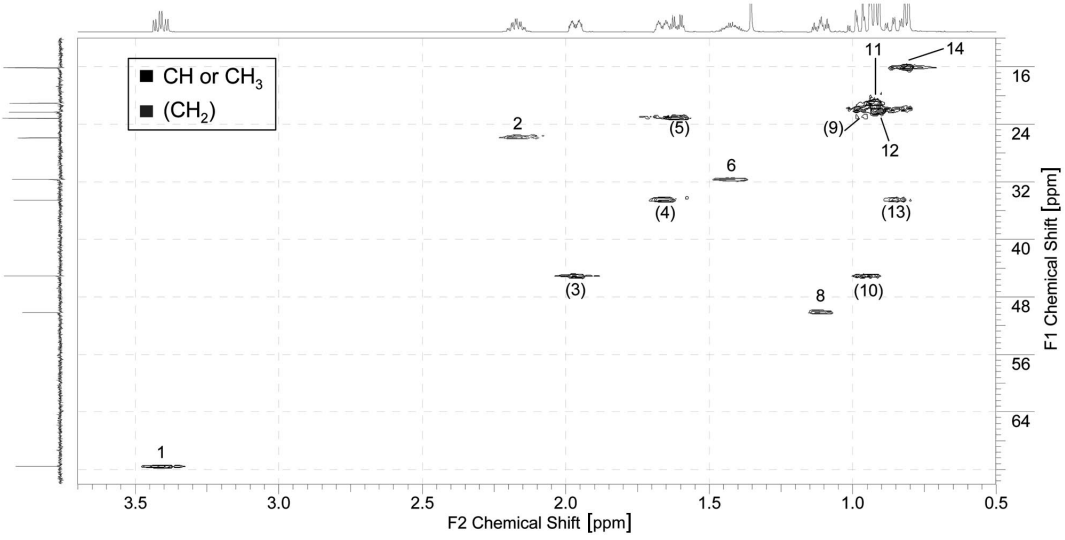

Figure 2. The HSQC spectrum of menthol assigns each proton to its directly attached carbon. H(9)–H(14), which clearly overlap in the 1D ^{1}H NMR spectrum, are clearly separated here, whereas methylene pairs CH_2(3, 10), CH_2(4, 13), and CH_2(5,9) are readily identifiable. The 1D ^{13}C NMR spectrum (F1 axis) is shown for clarity, but is not required for interpretation. Labels: proton ID. Phases: CH or CH_3 (black, no parentheses), CH_2 (gray, labels in parentheses).

Table 2. NMR data for menthol ($CDCl_3$).

ID	δ [ppm]		# of Hs	Type	Multiplet Structure		Connectivity Correlations	
	^1H	^{13}C			Type	Couplings [Hz]	HMBC [ppm]	COSY-45[b]
1	3.41	71.53	1	CH	td	10.4×2, 4.3	23.10, 25.82, 31.62, 45.03, 50.12	3, 8, 10
2	2.17	25.82	1	CH	sd[a]	7.1×6, 2.9	16.07, 21.00, 23.10, 50.12, 71.53	8, 11, 14
3	1.97	45.03	1	CH_2	dddd	12.1, 3.8×2, 2.1	22.20, 31.62, 34.51, 50.12, 71.53	1, (4), 6, 10
4	1.66	34.51	1	CH_2	dddd	3.4×2, 6.1, 12.4	23.10, 31.62, 45.03, 50.12, 71.53	(3), 9, 13
5	1.61	23.10	1	CH_2	dq	12.9, 3.3×3	31.62, 34.51, 50.12, 71.53	8, 9, 13
6	1.43	31.62	1	CH	m	(complex multiplet)	22.20, 34.51, 45.03	3, 12
7	1.35	–	1	exch.	br. s	–	–	–
8	1.11	50.12	1	CH	dddd	12.1, 10.3, 3.2×2	16.07, 45.03, 71.53	1, 2, 5
9	0.97	23.10	1	CH_2	m	(overlap)	34.51, 50.12	4, 5
10	0.95	45.03	1	CH_2	m	(overlap)	22.20, 71.53	1, 3
11	0.92	21.00	3	CH_3	d	7.4	16.07, 25.82, 50.12	2, (14)
12	0.91	22.20	3	CH_3	d	6.9	31.62, 34.51, 45.03	6
13	0.84	34.51	1	CH_2	dddd	12.4×2, 3.2, 1.1	(overlap)	4, 5
14	0.81	16.07	3	CH_3	d	7.1	21.00, 25.82, 50.12	2, (11)
Quaternary carbon atoms: none								

[a] Septet of doublets. [b] Long-range couplings are indicated with parentheses.

protons corresponding to each group is determined from 1D ^1H NMR integrations and HSQC phases, whereas proton–proton coupling constants can be extracted rapidly from first-order multiplets by using the method described by Hoye.[25] Correlations from other experiments are stored in additional columns. To avoid bias, one should adopt the convention of impartially recording a full data set (HSQC, COSY, HMBC; see below) before attempting analysis. The experimental parameters and chain of reasoning used to establish the proposed structure should also be recorded for future reference.

2.4. Homonuclear Correlation Spectroscopy (COSY, TOCSY)

With every proton uniquely identified, the next task is to deduce the structures of small fragments by using COSY to identify the relationships between protons on adjacent carbon atoms (vicinal couplings). In the COSY-45 experiment,[26] an improved[27] version of the more widely used COSY-90 experiment (see Figure S12 for a comparison), each peak represents a through-bond coupling between two protons. Typically, all geminal, many vicinal couplings, and some long-range couplings will appear. Because HSQC identifies methylene pairs, geminal couplings can be immediately removed from consideration. Long-range couplings can also be identified by their low intensity. In addition, they tend to be more visible on the F2 side of the diagonal.[28] Thus, vicinal couplings can be identified by elimination, allowing the construction of structural fragments (see below for examples).

TOCSY (total correlation spectroscopy), a related technique, is particularly useful in two situations: revealing isolated spin systems (particularly useful in polysaccharides and peptides) and simplifying overlapping spectra. In its most useful variant, 1D-DPFGSE-TOCSY (double pulsed-field gradient spin echo),[29] a "spin–lock" transfers magnetization from a selected proton to other protons in the same spin system. In many cases, increasingly remote protons are revealed by setting longer mixing times. This provides a quick method of assessing the proximity of two resonances (Figure 3).[30] The resulting 1D ^1H NMR subspectrum only shows protons from the same spin system, often removing the interference of overlapping peaks. Unlike COSY cross peaks, TOCSY correlations can be observed between two protons that have no significant J coupling. Highly sensitive, 1D-TOCSY requires no special calibrations and gives excellent resolution. It can be performed in less than five minutes, even with a dilute sample. Occasionally, minor phase distortions will appear and can be ameliorated by displaying the spectrum in absolute value mode.

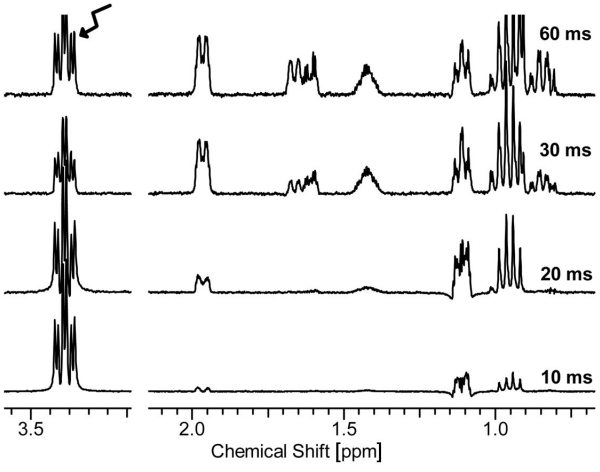

Figure 3. 1D-DPFGSE-TOCSY irradiation of H(1) in menthol. The extent of magnetization transfer depends on mixing time: 10 ms, 3 bonds; 20 ms: 4; 30 ms: 5; 60 ms: near-complete transfer.

2.5. Multiple-Bond Heteronuclear Correlation (HMBC, CIGAR)

Once several structural fragments have been deduced, they can be combined to establish the overall skeletal connectivity. The HMBC (heteronuclear multiple-bond corre-

lation) experiment is ideal for this purpose.[31] In this absolute-value 2D experiment (one proton and one carbon axis), each peak represents a proton within two or three bonds of a carbon atom. Correlations are often transmitted through intervening heteroatoms and quaternary carbon atoms. Therefore, this method can connect fragments whose termini have no visible COSY cross peaks (for example, the termini protons could reside in separate spin systems, have small proton–proton couplings for conformational reasons, or be obscured by spectral overlap). In addition, it can confirm or supplement COSY data for fragment generation. In menthol, the observation that CH_3(11) and CH_3(14) have mutual correlations indicates the presence of an isopropyl fragment.

Although HMBC is significantly less sensitive than HSQC, requiring 2–4 h under typical conditions (defined in Section 2.2), survey spectra can still sometimes be obtained in 30 min. Regardless of spectral quality, small pairs of peaks will often appear on either side of strong signals (Figure 4). These one-bond correlation artifacts appear at the chemical shift of their parent carbon atom, but are split along the proton axis by $^1J_{C,H}$ (120–250 Hz; mean: 140 Hz). Aromatic or conformationally rigid systems will occasionally show weak four- or five-bond couplings, particularly when the proton and carbon atoms are separated by coplanar bonds,[32] whereas geminal couplings to sp^2 carbons and *gauche* vicinal couplings to axial protons in fused cyclohexanes are often weak or missing. The absence of expected correlations is common and cannot be construed as evidence for or against a proposed structure.

The CIGAR (constant-time inverse-detected gradient accordion rescaled) variant of HMBC is a useful alternative for unknowns possessing closely spaced ^{13}C resonances.[33] Although it improves the suppression of one-bond artifacts, detects a wider range of correlations, and gives higher resolution spectra, it should only be used if HMBC is unsatisfactory because of its significantly reduced sensitivity (Figure S10). By contrast, ^1H–^{15}N HMBC is a practical and powerful source of information for alkaloids, despite the fact that it is approximately five times less sensitive than ^1H–^{13}C HMBC.[34]

2.6. Example: Structural Connectivity of Menthol

Menthol provides a simple example of the process of deducing the structural connectivity by generating fragment structures (Figure 5). Although fragments can be generated from any starting point, methyl groups, olefins, and carbonyls are usually good starting points. In the following, let $CH_3(m, n)$, $CH_2(m_1, m_2, n)$, $CH(m, n)$, and $C(n)$ denote particular methyl groups, methylene pairs, methines, and quaternary carbon atoms, respectively, where m_i and n denote proton identifiers and carbon chemical shifts, respectively.[18]

Menthol has a molecular formula of $C_{10}H_{20}O$ (one degree of unsaturation). Its 1D ^1H NMR spectrum suggests the presence of one aliphatic alcohol moiety (Figure 1). Beginning with the methyl groups, note that both CH_3(11) and CH_3(14) share a vicinal COSY correlation to CH(2) (identified by HSQC as a methine). This suggests a diastereotopic isopropyl fragment, a supposition confirmed by the mutual HMBC and long-range COSY correlations between CH_3(11) and CH_3(14). CH(2) has a further vicinal COSY coupling to H(8) (HSQC identifies this as a methine), suggesting fragment **7**. CH(8) has additional vicinal COSY correlations to CH(1) and H(5), a member of CH_2(5,9). The downfield nature of CH(1) indicates an adjacent oxygen atom. Because menthol has exactly one oxygen atom, this must correspond to OH(7), as shown in fragment

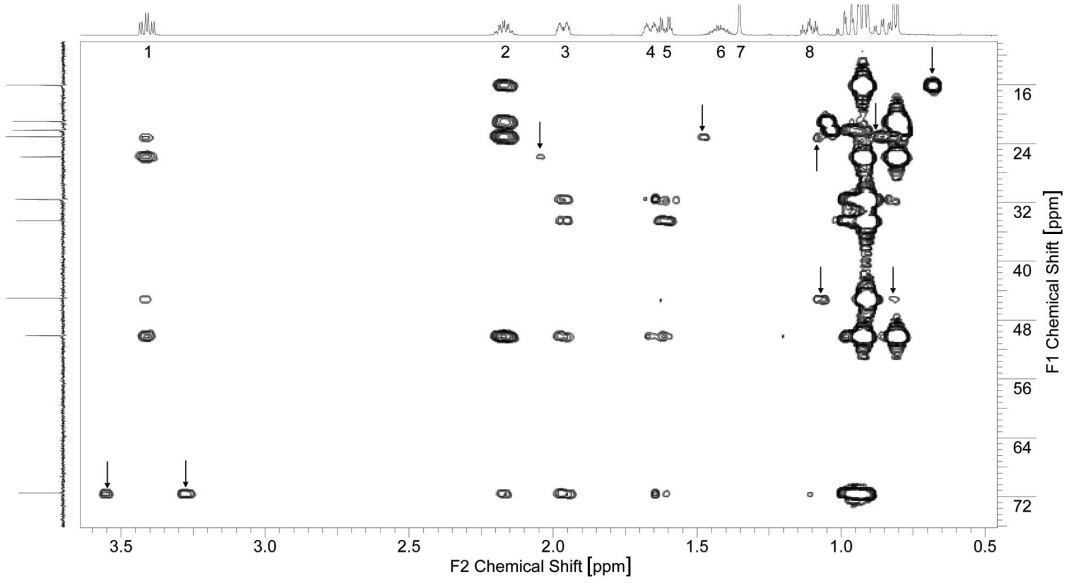

Figure 4. HMBC spectrum of menthol. Each peak is a proton bonded to a carbon atom two or three bonds away. Some of the spurious one-bond doublets ($J = {}^1J_{C,H}$) are marked with arrows. At lower contour levels, many more correlations (and artifacts) are visible.

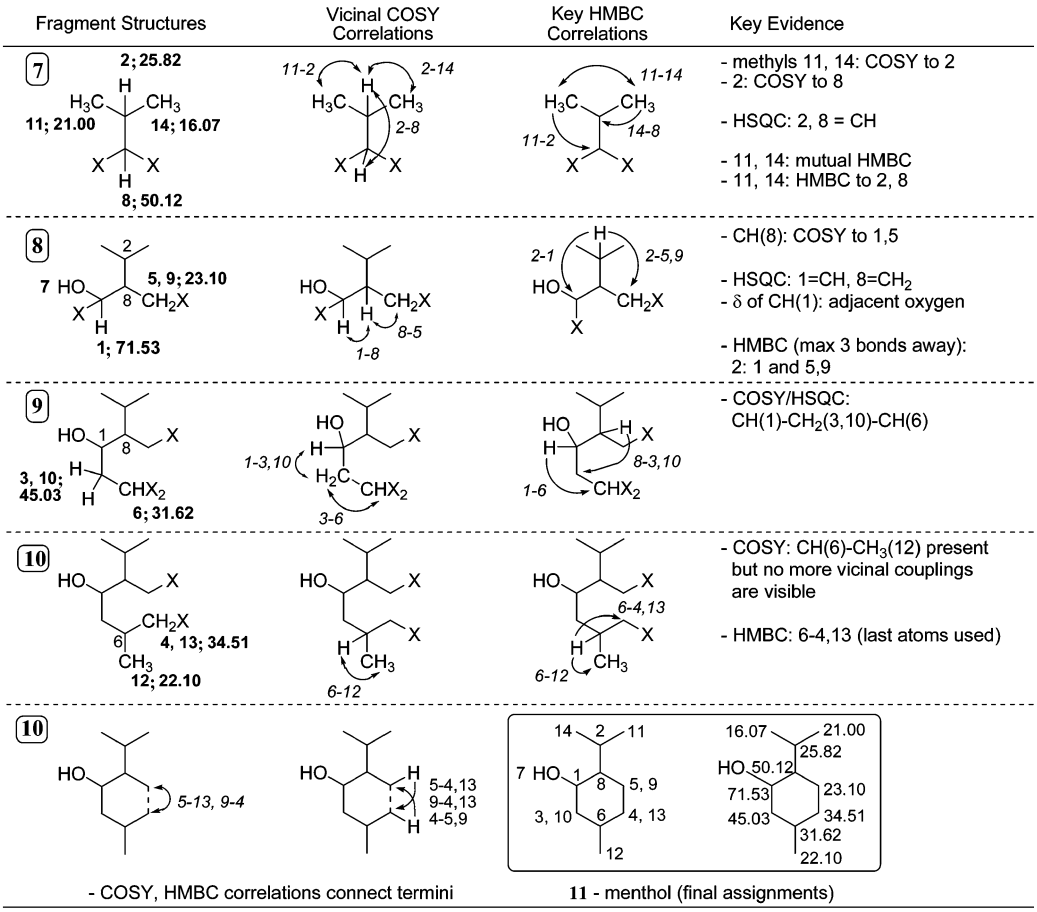

Figure 5. Fragment assembly for menthol. Numbers denote proton identifiers and carbon chemical shifts.

8. This connectivity is confirmed by HMBC correlations CH(2)–CH(1; 71.53) and CH(2)–CH_2(5,9; 23.10). CH(1) has further vicinal COSY correlations to CH_2(3,10), which in turn has a vicinal correlation to CH(6). The connectivity in updated fragment **9** is supported by HMBC correlations CH(8)–CH_2(3,10; 45.03) and CH(1)–CH(6; 31.62). CH(6) has a vicinal COSY correlation to CH_3(12), but further correlations are obscured by spectral overlap. However, CH(6) has an HMBC correlation to CH_2(4,13; 34.51), indicating fragment **10**. This incorporates all the atoms in the molecule. The unknown termini can then be joined to give **11**, the correct structure of menthol.

3. Determining Relative Stereochemistry

3.1. Nuclear Overhauser Effect (NOE)

In 1977, the availability of 270 MHz spectrometers allowed the 1D ^{1}H NMR spectrum of vancomycin, a glycopeptide antibiotic of considerable medicinal importance, to be partially assigned in terms of structural units found during chemical degradation.[35] During the course of this work, it was observed that when certain resonances were selectively irradiated (for "homonuclear decoupling"; see section 3.2), the intensity of spatially proximal resonances was reproducibly attenuated. This phenomenon, in which the irradiation of one resonance changes the intensity of nearby resonances, is known as the NOE and is a powerful method for determining relative stereochemistry. For example, further NOE experiments revealed that the stereochemistry of the atropisomeric diaryl ether region, previously assigned by analogy to that determined for the degradation product CDP-I was incorrect.

Of course, the determination of absolute stereochemistry is also an important task. Although the derivitization of chiral alcohols and amines with Mosher's reagent, α-methoxy-α-trifluoromethyl-α-phenylacetic acid (MTPA), has been the most widely used method, many other protocols are now available. As these methods were recently considered in a comprehensive review,[36] the following only discusses the determination of relative stereochemistry.

NOE correlations are ideal for establishing 1,3-stereochemical relationships in cyclohexanes; for example, the H(1)–H(6) correlation in menthol establishes a 1,3-*syn* relationship between the methyl and alcohol groups. It is less suitable for establishing 1,2-relationships because the observation of an NOE between adjacent cyclohexane protons could be consistent with either a *syn* or an *anti* disposition. However, it is helpful in distinguishing between *E* and *Z*

olefins and *exo* and *endo* Diels–Alder adducts. Complex structures whose conformations may deviate from textbook geometries should be analyzed with molecular modeling.

The DPFGSE-NOESY experiment is an efficient method for observing the NOE.[37] In its 1D variant (one proton axis), one proton resonance is selectively irradiated and NOE correlations are observed as oppositely phased peaks (Figure 6). It is highly sensitive and requires approximately five minutes under typical conditions (defined above). This experiment gives significantly fewer artifacts than the traditional NOE difference experiment. Correlation intensities are often asymmetrical (i.e., proton A to proton B has a different intensity to that of B to A) and without calibrations give only a qualitative measure of distance; typically, the level of enhancement is reported as strong, medium, or weak. In its phase-sensitive 2D variant (two proton axes), all correlations are sampled and appear as off-diagonal cross peaks; here, the diagonal is negatively phased and cross peaks are positively phased. Although this requires significantly more experimental time, closely spaced peaks are distinguished more readily.

The intensity of NOE correlations is heavily influenced by molecular weight and the choice of mixing time.[38] Very small molecules (MW $<$ 200 Da) have inherently weak NOE correlations, and may require the increased sensitivity of the 1D-NOESY sequence for detection. Intermediate-sized molecules (MW $>$ 750 Da) can give very weak or even negative NOE intensities and are best analyzed by using the transverse DPFGSE-ROESY (rotating frame NOESY) sequence.[39] Also available in 1D and 2D forms, this experiment is operationally identical to the NOESY experiment, but shows all correlations as positive peaks, regardless of molecular weight. Mixing times are typically chosen to be between 0.3 and 0.6 s. Mixing times must be long enough to allow sufficient time for NOE correlations to build up, while being short enough to prevent signal loss due to relaxation. In comparison to smaller molecules, larger molecules have NOE correlations that build up faster and magnetizations that relax faster. In addition, ROESY correlations build up twice as fast as NOESY correlations; therefore, large molecules require shorter mixing times than small ones (Table 1).

The most common artifacts in NOESY and ROESY spectra are due to COSY transfer or chemical exchange (Figure 6). COSY correlations appear with a characteristic alternating phase and are common when two protons share a large vicinal diaxial coupling.[40] Chemical exchange peaks appear with negative phase and occur when the exchanging protons have a lifetime comparable to the mixing time. At high concentrations, intermolecular NOE correlations can appear.

3.2. Proton–Proton Coupling Constants[41]

The value of $^{n}J_{H,H}$ varies with conformation according to the Karplus relationship in a highly reliable manner.[42] In particular, vicinal couplings, $^{3}J_{H,H}$, are well suited to the identification of 1,2-stereochemical relationships in cyclohexanes, olefins, and cyclopropanes, and rigid fused ring systems, whereas $^{4}J_{H,H}$ values are usually too small to give information about 1,3-stereochemical relationships. Caution must be used when analyzing five-membered rings and other conformationally flexible systems because averaging may allow two diastereomers to have very similar coupling constants. Nonetheless, $^{3}J_{H,H}$ values and NOE/ROE correlations give very useful and complementary information. For example, in menthol, CH(8) has four couplings: 12.1, 10.3, 3.2 × 2 Hz. To identify their origins, note the following: methines cannot have geminal couplings, isopropyl CH(2) shows a ≈ 3 Hz coupling to H(8), and CH(8) must share one small *gauche* and one large *anti* coupling with its adjacent methylene protons. Thus, CH(8) and CH(1) must share a large 1,2-diaxial coupling. This is confirmed by the couplings of CH(1), 10.4 × 2, 4.3 Hz: one large and one small coupling to its adjacent methylene and one large 1,2-diaxial coupling to CH(8). With the strong H(6)–H(1) NOE correlation establishing a 1,3-*syn* relationship between the methyl and alcohol groups, the correct stereochemistry of menthol (**11**) is clear.

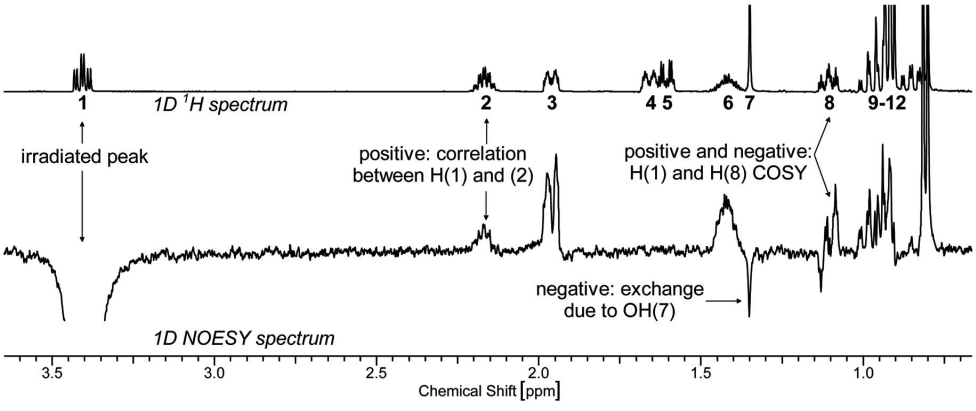

Figure 6. 1D NOESY spectrum of menthol. Positive peaks indicate through-space correlations between two protons. Note that real NOE correlations appear alongside exchange and COSY artifacts, which have readily identifiable phases.

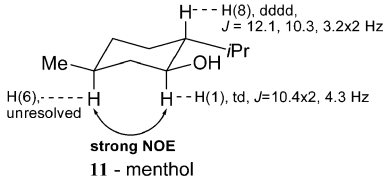

11 - menthol

The easiest way to obtain values of $^{n}J_{H,H}$ is to extract them directly from first-order multiplets by using the efficient procedure reported by Hoye and coworkers.[25] When spectral overlap or strongly coupled spectra (see below) precludes direct extraction, the simplest solution is to obtain 1D ^{1}H NMR spectra in different solvents (J values generally remain constant between solvents unless hydrogen bonding is involved).[15] 1D ^{1}H NMR subspectra, obtained by taking slices along the proton (F2) axis of HSQC spectra, can give estimates of the relative size of couplings (Figure 7). This method is well suited to distinguishing the axial and equatorial protons of methylene pairs in cyclohexanes; for example, in menthol, $H_{eq}(3)$ appears as a doublet, whereas $H_{ax}(9)$ appears as a quartet. This works because only large couplings appear within such subspectra: equatorial protons contain only one large geminal coupling, whereas axial protons can contain large diaxial couplings as well. However, the size of the couplings measured by using this method tend to be unreliable.

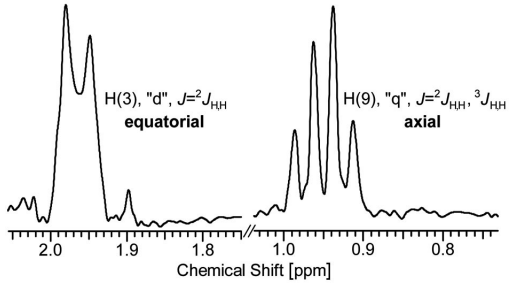

Figure 7. A slice along the proton axis (F2) of the HSQC spectrum of menthol. Peaks only show large couplings, allowing axial and equatorial protons to be distinguished.

A more accurate approach is to use 1D-TOCSY to selectively irradiate a clearly resolved proton that lies in the same spin system as an obscured one.[43] For example, irradiation of H(1) in menthol clearly shows adjacent and previously overlapping H(9) as an approximate quartet with coupling constant 11.6 Hz (Figure 3, 20 ms), a result consistent with the corresponding HSQC subspectrum. In general, a mixing time of 20 ms will limit TOCSY transfer to three bonds.

When a proton has too many couplings to be well resolved, homonuclear decoupling can sometimes simplify its appearance.[44] In principle, this technique gives a 1D ^{1}H spectrum in which all couplings to a selected proton have been removed. The result is that complex multiplets can collapse into simpler ones whose coupling constants can be measured; for example, homonuclear decoupling of H(2) in menthol removes the corresponding 3 Hz coupling from H(8), producing a ddd (J = 12.2, 10.2, 3.4 Hz), an observation consistent with the previously extracted coupling constants (Figure 8). This technique only works in some cases because the decoupled spectra can remain too complex or contain distortions; for example, homonuclear decoupling was unable to simplify H(6) enough for direct analysis.

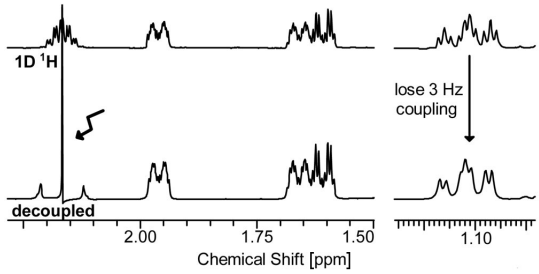

Figure 8. Simplification of multiplets with homonuclear decoupling.

Alternatively, couplings can be determined by using phase-sensitive COSY techniques such as DQF-COSY (double quantum-filtered COSY)[45] or E-COSY (exclusive COSY).[46] In these experiments, adjacent components of a particular cross peak appear with alternating phase. In principle, the spacing between components corresponds to the active coupling.[47] However, protons can have many small long-range couplings in addition to large geminal and vicinal couplings, giving rise to complex multiplet patterns. If unresolved, their presence can significantly complicate analysis. Consequently, these COSY experiments may require much more experimental time than COSY-90 or COSY-45 would.

Caution should be exercised when extracting coupling constants from multiplets whose coupled partners are close in chemical shift. For example, suppose $^{3}J_{A,X}$ is being used to distinguish between epimers **12a** and **12b** in the typical ABX system shown below (assume there are no protons on R). Normally, one large (8 to 13 Hz) and one small (0 to 6 Hz) coupling constant would indicate **12a**, whereas two small coupling constants would indicate **12b**.

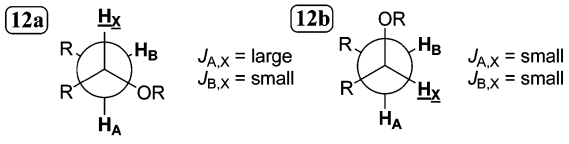

However, as the chemical shift difference ($\Delta\nu$) between A and B decreases relative to $J_{A,B}$, the apparent and real couplings can deviate significantly (see Figure 9; typically, deviations become apparent when $10\Delta\nu < {}^{n}J_{H,H}$). In this example, distortions first appear as a "roof effect" (Figure 9a). In the limit that $\Delta\nu = 0$, H_X becomes an apparently misleading triplet (J = 6.0 Hz), despite its actual couplings of 9.0 and 3.0 Hz (Figure 9d). In general, multiplet spacings in "second-order spectra" do not correspond to the actual couplings in any simple way ("virtual coupling"); in fact, it is even possible to observe many more lines than expected.[49] This situation often arises in complex molecules and can be detected by changing the magnetic field strength: higher-order multiplets appear increasingly anomalous at lower field strengths. Coupling constants can be

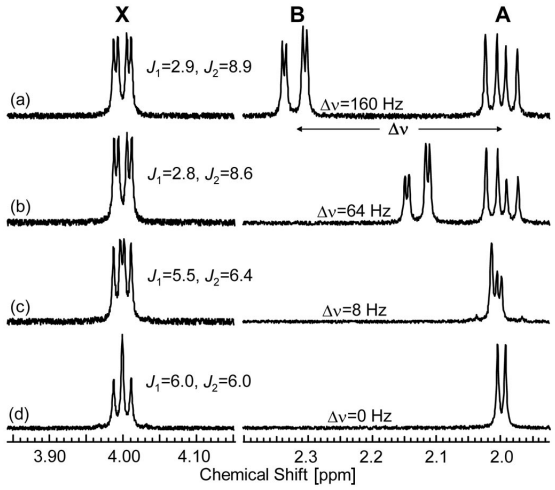

Figure 9. Virtual coupling can significantly affect apparent coupling constants. Shown: simulated spectra[48] for an ABX system and their apparent coupling constants [Hz]. As the chemical shift of B approaches that of A, deviations increase: (a) $\Delta\nu/J_{A,B}$ = 10, slight roof effect; (b) $\Delta\nu/J_{A,B}$ = 4, significant roof effect; (c) $\Delta\nu/J_{A,B}$ = 0.5, major distortion, misleading couplings; (d) $\Delta\nu/J_{A,B}$ = 0, apparent couplings are average of actual couplings. Simulation parameters: $\delta(H_X)$ = 4.00 ppm, $\delta(H_A)$ = 2.00 ppm, $J_{A,B}$ = 16 Hz, $J_{B,X}$ = 3 Hz, $J_{A,X}$ = 9 Hz, 500 MHz spectrometer, 2 Hz linewidth.

laboriously extracted from such second-order spectra by computer simulations or obtained from solvent-shifted spectra. Fortunately, neither HETLOC nor TOCSY measurements of $^nJ_{C,H}$ (discussed below) suffer from this problem because one proton is always bonded to ^{13}C (the large $^1J_{C,H}$ coupling effectively removes the chemical shift equivalence).

3.3. Proton–Carbon Coupling Constants

Until recently, the use of $^nJ_{C,H}$ values for structural elucidation was relatively uncommon because the best method of measuring $^nJ_{C,H}$ was to obtain nondecoupled 1D ^{13}C NMR spectra of isotopically enriched compounds.[50] Newer, more sensitive methods allow the use of natural abundance samples by detecting proton, rather than carbon, magnetization ("inverse detection").[51] The stereochemistry of many acyclic chains, for which $^nJ_{H,H}$ and NOE measurements alone are inconclusive, can be elucidated by using $^nJ_{C,H}$ values.[52] The magnitude, sign, and conformational dependence of proton–carbon couplings is similar to that of proton–proton couplings (Figure 10a).[53] Geminal couplings ($^2J_{C,H}$) are usually negative, whereas vicinal couplings ($^3J_{C,H}$) are usually positive (the sign[54] of a coupling constant reflects whether the two spins are more stable when paired or opposed).[55] In cyclic systems, $^nJ_{C,H}$ can give information about both 1,2- and 1,3-stereochemical relationships; for example, in menthol, $^2J_{C(71.53),H(8)}$ = –6.3 Hz, indicating a 1,2-*anti* relationship between the isopropyl and alcohol groups, whereas $^3J_{C(71.53),H(6)}$ =

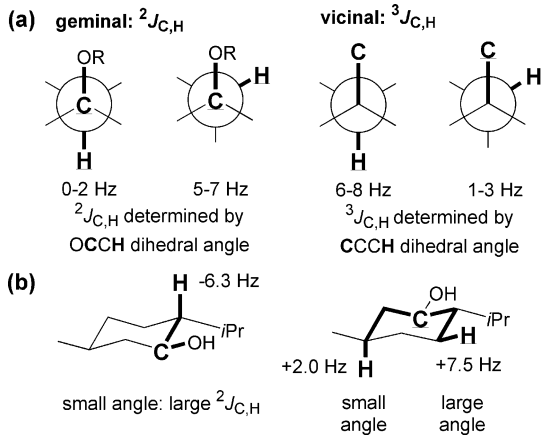

Figure 10. (a) Dependence of carbon–proton coupling constants on conformation; (b) selected C,H coupling constants (HETLOC) in menthol.

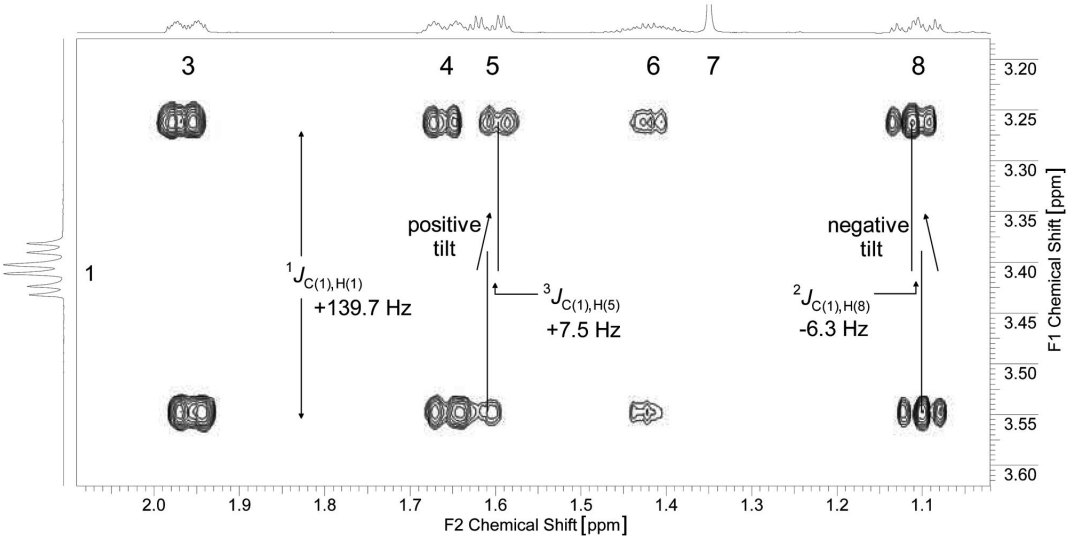

Figure 11. H(1) region of the HETLOC spectrum of menthol. The horizontal displacement of each doublet represents $^nJ_{C,H}$. The sign of the couplings is given by the direction of slant relative to the diagonal for each pair of peaks, often allowing geminal and vicinal couplings to be distinguished.

+2.0 Hz, indicating a 1,3-*syn* relationship between the alcohol and methyl groups (Figure 10b).

The HETLOC (heteronuclear long-range coupling) experiment described by Uhrín and coworkers is a robust and sensitive method for measuring $^{n}J_{C,H}$.[56] This phase-sensitive 2D experiment (two proton axes) shows generally the same cross peaks (all positively phased) as a COSY spectrum. Each cross peak appears as a doublet split by $^{1}J_{C,H}$ along F1 and $^{n}J_{C,H}$ along F2 (Figure 11). Because $^{1}J_{C,H} >> {}^{2,3}J_{C,H}$ (≈ 140 vs. 5 Hz, on average), each doublet is widely separated in F1 and slightly separated in *F*2. This method can only measure a coupling between a protonated carbon and a proton residing in the same spin system. As such, it cannot measure couplings to, or through, quaternary carbon atoms (other methods, not discussed here, can measure these couplings; unfortunately, these methods are less sensitive[51]). The tilt of each pair relative to the diagonal can distinguish between geminal and vicinal couplings by indicating the sign of the coupling; for example, a pair of peaks tilted opposite to the diagonal indicates a negative coupling (the diagonal only contains $^{1}J_{C,H}$ couplings, which are always positive). A key part of the experiment incorporates a TOCSY-type mixing time of user-defined length. In general, a mixing time of 20 ms will show most geminal and vicinal couplings. Longer mixing times can substantially increase spectral complexity and reduce the signal-to-noise ratio.

An alternative method, suitable for quickly measuring a few $^{n}J_{C,H}$ values, was recently reported by Espinosa and coworkers.[57] In this technique, a 1D ^{1}H NMR spectrum is examined to identify the ^{13}C satellites of a peak of interest. The 1D-TOCSY sequence is then used to irradiate these satellites separately and selectively. Coupling constants are extracted by measuring the different positions of the TOCSY correlations in the two spectra (for details, see Figure S11). This approach appears to give good results within one hour for samples as dilute as 15 mM and is appealing because it is simple and can quickly resolve a given stereochemical ambiguity. It requires that the ^{13}C satellites of the peak of interest be separated from other peaks and visible within several scans. As before, couplings to, or through, quaternary carbon atoms cannot be measured this way.

4. Verifying Proposed Structures

Although NMR methodology is now useful for the elucidation of even the most intricate small molecules, the complexity of the required data analysis requires that any proposed structure be verified rigorously. In some cases, proposed structures can be corroborated by single-crystal X-ray analysis. However, single crystals are often unavailable, and in rare cases, X-ray structures have been found to be incorrect (e.g., diazonamide A[58]). Indeed, the structures of many natural products have been revised or placed under reconsideration in light of additional evidence. Such evidence can take many forms; for example, dissimilar additional members of a family of natural products might be isolated and render a proposed structure inconsistent with a proposed common biosynthetic scheme. More often, total synthesis has revealed inconsistencies between proposed structures and natural materials. Even today, synthesis remains the gold standard for the proof of a proposed structure. In the following, we discuss common strategies for structural verification and highlight some high-profile examples of incorrectly elucidated natural products.

At a basic level, several steps should be taken to avoid errors: each entry in the data table should be checked; every inference should be recorded and supported by more than one data point; and once a structure has been proposed, the entirety of the data should be reexamined to ensure that there are no inconsistencies. Indeed, significant errors can occur when contradictory data are ignored in an attempt to fit observations to a preconceived structure. For example, the structure of the natural product hexacyclinol was originally thought to be endoperoxide **12**.[59] However, computations[60] later suggested that the chemical shifts were more consistent with bis(epoxide) **13**, a hypothesis that was recently confirmed by total synthesis.[61] An analysis of the original report[62] suggests that at least three errors were made: H(12) is located at δ = 3.62 ppm, not 3.55 pm; H(12) is directly attached to a carbon atom at δ = 41.0 ppm, not 40.4 ppm; and H(19) is directly attached to a carbon atom at δ = 40.6 ppm, not 40.9 ppm. These errors likely resulted from insufficient carbon resolution in the original heteronuclear correlation spectra.[63] In retrospect, the chemical shifts of **12** seem unusual, even without computations (Figure 12). Although very useful, empirical knowledge of chemical shifts should be used in conjunction with other data, because atoms in unusual chemical environments can experience misleading chemical shifts. Fortunately, commercially available computer programs can not only accurately predict chemical shifts, but also independently propose structures given an NMR spectroscopic dataset.[64]

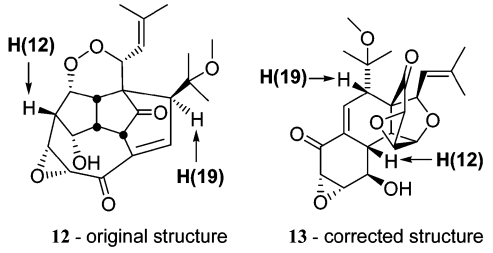

Figure 12. Structures of hexacyclinol. The chemical shifts are clearly more consistent with **8**: 3.62 [s, H(12)], 3.59 [d, *J* = 5.3 Hz, H(19)] ppm.

One structure currently under reconsideration is that of palau′amine, a marine natural product with purported anticancer activity. Crucial to the original *cis* assignment (**14**) was the 14.1 Hz coupling between H(11) and H(12). Although this is a rather large value for a *cis*-fused bicyclo[3.3.0] system, an analogy was made to leucodrine,[65] another spiroannulated five-membered ring (**18**). Although neither X-ray analysis nor total synthesis has yet been possible, the recent isolation of related compounds tetrabromo-

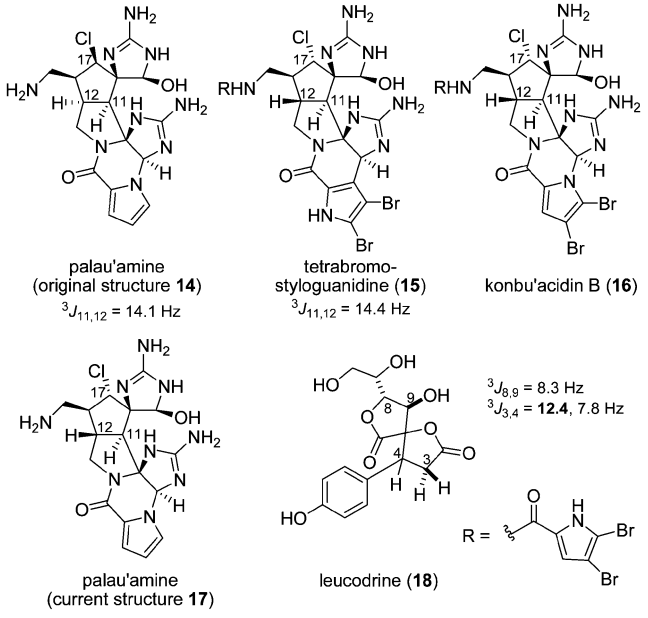

styloguanidine (**15**) and konbu′acidin B (**16**) has led to the proposal that **17** is the correct structure of palau′amine.[66] Compound **17** possesses an unusual and energetically less preferable (calculations: 27.3 kJ mol^{-1}) *trans*-, rather than *cis*-, five-membered ring fusion. The *trans* assignment of **15** stems from the predicted size of $^3J_{11,12}$: 13.1 Hz and 14.6 Hz for the *cis*- and *trans*-fused isomers, respectively. Because the experimental value is 14.4 Hz, the fusion was assigned as *trans.* Detailed quantitative ROESY measurements further verified this assignment. The hypothesis that the other alkaloids in this family should be similarly reassigned is supported by the current proposal for their biosynthetic origin.[66]

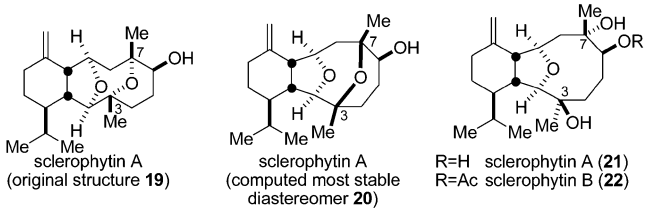

The case of sclerophytin A, a diterpene isolated from a soft coral, is noteworthy for the roles that both spectroscopy and synthesis played in its elucidation. Although initially proposed to be **19** [note the confusing stereochemical descriptors at C(3)],[67] both the original spectroscopic data and subsequent X-ray and CD data are equally compatible with **20**. Because computational studies suggested that **20** is by far the most stable of all the possible C(3)/C(7) diastereomers of **19**, synthesis efforts were initiated towards **20**.[68] Unfortunately, neither the chemical nor the spectroscopic behavior of **20** matched that of sclerophytin A. A reevaluation of the original isolates[69] soon revealed two significant discrepancies: a molecular formula of $C_{22}H_{36}O_5$, not $C_{22}H_{34}O_4$ (NMR, CI-MS, LC/ESI-TOF-MS) and the presence of hydroxy groups (IR) in sclerophytin B, the monoacetylated congener of sclerophytin A. With the aid of HMBC and other experiments, revised structure **21** was proposed. Note that **21** contains one, not two, ether bridges. This hypothesis was then confirmed by synthesis.[70]

Although the specifics of what led to the originally misleading mass spectroscopic data remain unclear, the original isolation workers apparently relied on the APT technique[19] to assign the 1D ^{13}C NMR peaks to methyl, methylene, methine, or quaternary carbon atoms.[18] Therefore, any protons that were not attached to carbon were missed. Had an HSQC spectrum been obtained, it might have been noticed that some protons had no corresponding carbon atom. Similarly, a close examination of NOESY spectra might have revealed the presence of negative correlations indicative of chemical exchange.

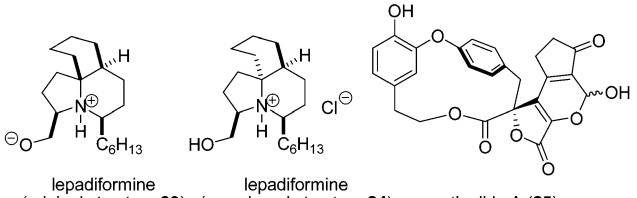

Lepadiformine, a marine alkaloid, presents a similar case where a structure based on misleading mass spectroscopic data was corrected by total synthesis.[71] In this case, confusion apparently arose because the original (and highly unusual) structure, zwitterionic amino alcohol **23**, and the corrected structure, hydrochloride salt **24**, have similar chemical shifts and identical molecular cations. As these examples illustrate, even the most meticulous NMR spectroscopic analysis can be stymied by an incorrect molecular formula. Therefore, the use of high-quality HRMS (high-resolution mass spectrometry), and if possible, elemental analysis data, are essential.

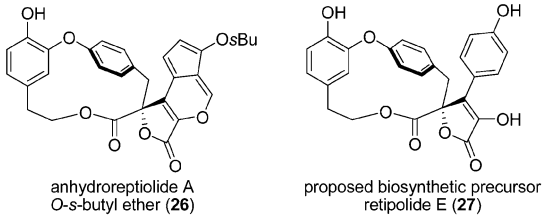

The recently reported elucidation of retipolide A (**25**), a fungal spiromacrolactone, by Steglich and coworkers represents a well-executed example of systematic structural elucidation and verification.[72] First, the molecular formula was obtained from EIMS. Next, structural fragments were assembled and combined from COSY and HMBC data, whereas the relative configuration was determined from NOE and proton–proton coupling constants. Finally, the structure was converted into anhydroreptiolide *O*-*s*-butyl ether **26**. Subsequent single-crystal X-ray analysis of **26** was consistent with the proposed structure.

Further efforts elucidated the structures of other members of the retipolide family. Because a biosynthetic consideration of their origin predicted a common precursor, retipolide E (**27**), additional plant extracts were prepared.

By using independently synthesized material for comparison, the extracts were purified by HPLC. The isolation of natural **27** then confirmed the biosynthetic proposal.

5. Case Study: Salvinorin A

The potent hallucinogen salvinorin A was isolated in 1982 from a rare Mexican mint.[73] Its unique biological activity as a κ opioid receptor agonist has made it the subject of recent biological[74] and synthetic[75] studies. Its analysis is complicated by the presence of a number of isolated spin systems, whose members nonetheless show many long-range COSY couplings. As a result, the use of HMBC is essential to establishing its structural connectivity.

An initial analysis reveals the following: a molecular formula of $C_{23}H_{28}O_8$ (MS and elemental analysis), a carbonyl IR absorption ($\tilde{\nu}_{max}$ = 1735 cm^{-1}), and considerable overlap and evidence of second-order effects in the aliphatic region of its 1D ^1H NMR spectrum (600 MHz, $CDCl_3$). Fortunately, the corresponding spectrum in $CDCl_3/C_6D_6/C_5D_5N$ (1:1:1) is relatively clear (Table 3).[76a] HSQC confirms the presence of 28 protons: eight methine, four pairs of methylene, and four methyl groups, leaving seven quaternary carbon atoms. HMBC (or 1D ^{13}C) shows a number of low-field resonances: C(202.36), a potential ketone; C(169.66), C(171.01), and C(171.75), potential esters or lactones; and CH(4, 143.79), CH(1, 139.72), C(125.95), CH(3, 108.80), two potentially polarized olefins. With 10 degrees of unsaturation, and the provisional assumption that 4 carbonyl groups and 2 olefins are present, it can be concluded that 4 rings are present.

A number of small preliminary fragments can quickly be generated. The HMBC correlations between singlet CH_3(6) and C(171.75) suggests methyl ester fragment **28**, whereas the correlation between singlet CH_3(13), appearing at δ = 1.90 ppm, and C(169.66) suggests acetate fragment **29**. CH_3(19) and CH_3(20), aliphatic singlets, have HMBC correlations to quaternary carbon atoms C(35.52) and C(42.04), suggesting methyl fragments **30** and **31**.

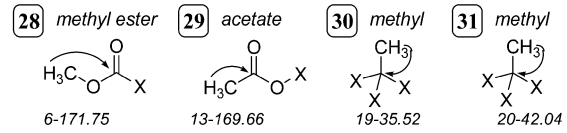

Of CH(1, 139.72), CH(2, 143.79), CH(3, 108.80), and C(125.93), identified above as parts of two polarized olefins, the former two are at relatively low field, whereas the latter two are at relatively high field. The network of COSY correlations suggest an H(1)–H(4)–H(3)–H(2) connectivity pattern. With each of H(1), H(2), and H(3) having proton chemical shifts above 6 ppm, it is reasonable to suggest the presence of a monosubstituted furan. Specifically, the high-field nature of C(125.93), the *ipso* carbon, indicates a 3-substituted furan. In addition, H(4), a doublet of doublets, has COSY and HMBC correlations to CH_2(8, 18, 43.11), suggesting an adjacent methylene unit. Finally, the downfield nature of H(4, 71.87) (δ = 5.26 ppm) suggests an additional electronegative substituent, identified by HMBC correlation H(4)–C(171.01) as an ester or lactone linkage. This gives fragment **32** (Figure 13).

Table 3. NMR data for Salvinorin A ($CDCl_3/C_5D_5N/C_6D_6$, 1:1:1).

ID	δ [ppm]		# of H	Type	Multiplet Structure		Connectivity Correlations		NOESY[a]
	^1H	^{13}C			Type	$J_{H,H}$ [Hz]	HMBC [ppm]	COSY-45	
1	7.17	139.72	1	CH	s	–	108.80	3, 4	4, 8
2	7.16	143.79	1	CH	t	1.5×2	125.93	3	3
3	6.15	108.80	1	CH	s	–	125.93, 139.72, 143.79	1, 2	2, 8
4	5.26	71.87	1	CH	dd	11.8, 5.1	43.11, 108.80, 125.93, 139.72, 171.01	1, 8, 18	1, 8, 19
5	5.12	75.38	1	CH	dd	12.5, 7.4	30.98, 169.66, 202.36	9, 10	7, (9), 10
6	3.44	51.66	3	CH_3	s	–	171.75	–	15, 20
7	2.61	53.24	1	CH	dd	13.3, 3.0	16.34, 30.98, 38.11, 42.04, 63.27, 75.38, 171.75	9, 10, 11	5, (9), 10
8	2.30	43.11	1	CH_2	dd	13.4, 5.1	15.16, 35.52, 51.09, 63.27	4, 18	1, 3, 4, 19
9	2.18	30.98	1	CH_2	q	13.0×3	42.04, 53.24, 75.38, 171.75, 202.36	5, 7, 10	(5), 10, 20
10	2.06	30.98	1	CH_2	ddd	13.1, 7.3, 3.3	42.04, 75.38, 171.75, 202.36	5, 7, 9	5, 7, 9
11	2.05	63.27	1	CH	s	–	15.16, 35.52, 42.04, 51.09, 202.36	7, 19, 20	14
12	2.01	18.50	1	CH_2	dq	14.1, 2.9×3	35.52, 38.11, 42.04, 51.09	14, 15, 16, 17	14, 16
13	1.90	20.48	3	CH_3	s	–	169.66	–	–
14	1.79	51.09	1	CH	dd	12.0, 2.6	15.16, 18.50, 35.52, 43.11, 63.27, 171.01	12, 16, 19	11, 12, (16)
15	1.54	38.11	1	CH_2	dt	13.3, 2.6×2	16.34, 18.50, 42.04, 51.09, 63.27	12, 16	6
16	1.46	18.50	1	CH_2	dq	13.3, 2.8×3	38.11, 42.04, 51.09	12, 14, 15	12, (14)
17	1.35	38.11	1	CH_2	dt	13.2, 3.4×2	(overlap)	(overlap)	(overlap)
18	1.33	43.11	1	CH_2	t	12.4×2	(overlap)	(overlap)	(overlap)
19	1.25	15.16	3	CH_3	s	–	35.52, 43.11, 51.09, 63.27	11, 14	4, 8, 20
20	0.90	16.34	3	CH_3	s	–	38.11, 42.04, 53.24, 63.27	11	6, 9, 19
Quaternary carbon atoms: 35.52, 42.04, 125.93, 169.66, 171.01, 171.75, 202.36									

[a] Spurious COSY correlations are indicated with parentheses.

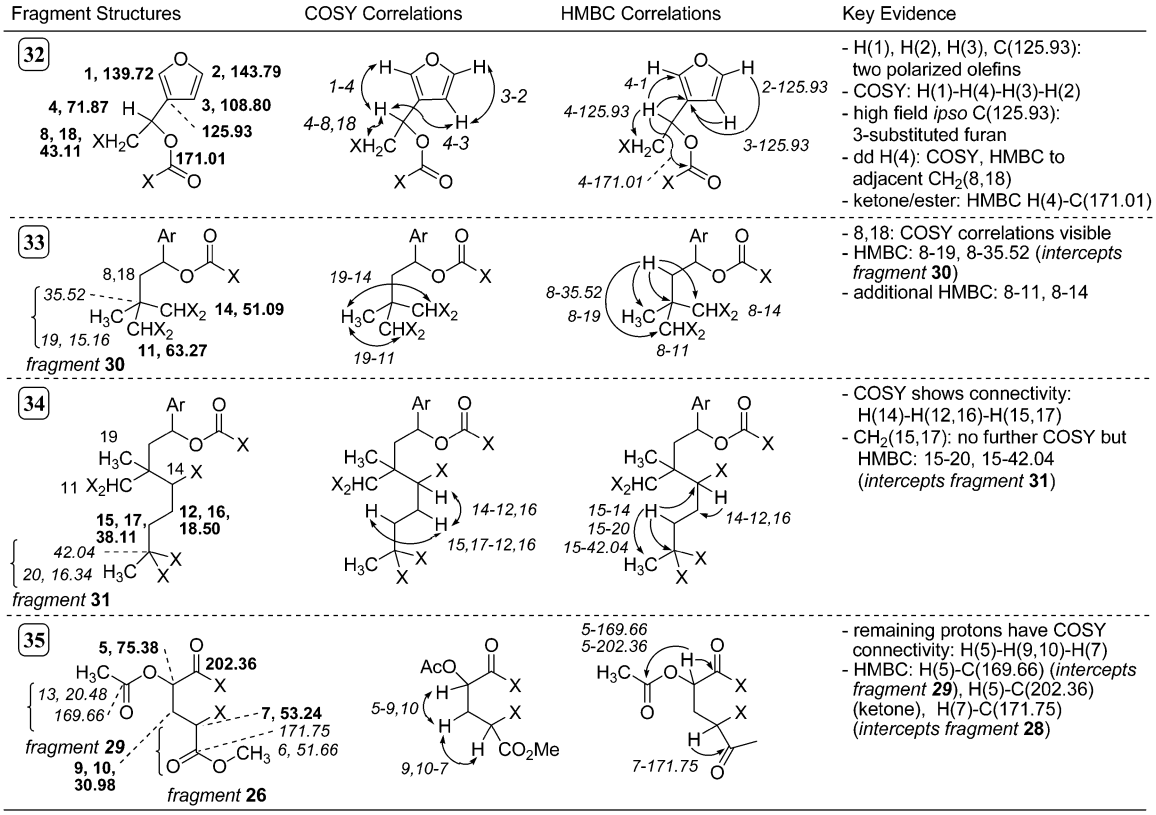

Figure 13. Fragment assembly for salvinorin A.

Although CH_2(8, 18) has no further COSY correlations, suggesting no adjacent protons, it does have HMBC correlations to C(35.52) and CH_3(19), intercepting fragment **30**. With additional HMBC correlations to CH(11, 63.27) and CH(14, 51.09), updated fragment **33** can be generated. Although H(11) has a COSY correlation to H(7), its appearance as a singlet suggests that this is a long-range coupling. By contrast, doublet of doublets H(14) has further COSY correlations, which suggest a CH(14)–CH_2(12,16)–CH_2(15,17) connectivity pattern. This pattern is supported by HMBC correlations H(14)–CH_2(12, 16, 18.50) and H(15)–CH(14, 51.09). As before, CH_2(15, 17) has no further COSY correlations but has HMBC correlations to C(42.04) and CH_3(20), intercepting fragment **31**. This generates fragment **34**. COSY correlations and coupling patterns suggest that the remaining protons, CH(5) (dd), CH_2(9, 10) (q, ddd), and CH(7) (dd) form an isolated spin system with connectivity as written. Selective 1D-TOCSY irradiation of CH(5) at successively longer mixing times confirms this hypothesis. The downfield nature of CH(5) (δ = 5.12 ppm) and its HMBC correlations to C(202.36) and C(169.66) suggest that its additional ligands are a ketone and acetate fragment **29**, respectively. Finally, the chemical shift of CH(7), 2.61 ppm, and its HMBC correlation to methyl ester C(171.75) intercept fragment **28**, generating fragment **35**.

With all the atoms assigned, all that remains is to connect the remaining unknown termini. Of the two possibilities, **36** and **37** (Figure 14), note that it is unlikely that CH(7) and CH(11) share a vicinal coupling [CH(11) is a singlet]. In addition, **36** would require several intense HMBC correlations to arise from four-bond couplings, whereas **37** would not. Thus, **37** gives the correct connectivity of salvinorin A.

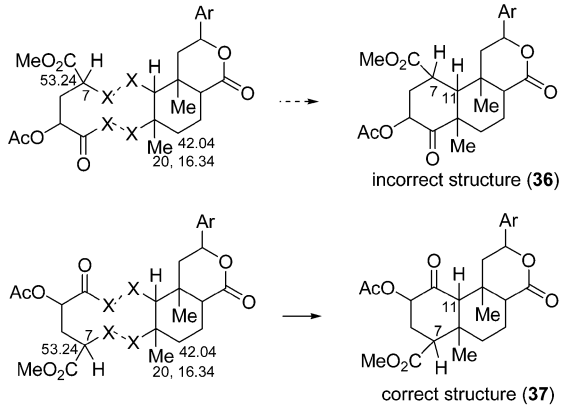

Figure 14. Connecting unknown termini. CH(11) appears as a singlet, precluding **36**. Intense HMBC correlations 7–16.34, 7–42.04, and 20–53.24 would be four-bond couplings in **36** but three-bond couplings in **37**.

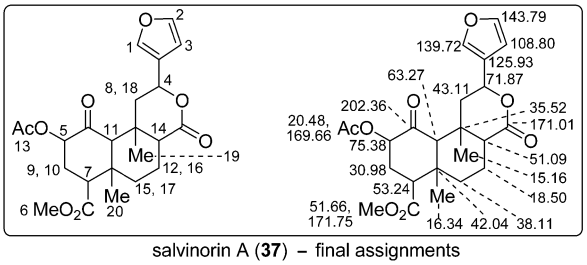

Within the cyclohexanone, the NOE correlation between H(5) and H(7) suggests a 1,3-*syn* relationship between the acetate and methyl ester. Because both H(5) and H(7) display one large and one small proton–proton coupling, and are therefore axial, both the acetate and methyl ester must be equatorially disposed. Similarly, H(9) displays three large couplings (one geminal, two 1,2-diaxial) and is also axial. With NOE correlations H(7)–H(11) and H(9)–H(20) establishing further 1,3-*syn* relationships, a *trans*-decalin ring fusion can be inferred.

To establish the stereochemistry of the lactone ring fusion, note NOE correlations $CH_3(20)$–$CH_3(19)$ and H(11)–H(14). These suggest the relative configuration depicted in Figure 15. Finally, the NOE correlation between $CH_3(19)$ and furylic CH(4) suggests a 1,3-*syn* relationship. These assignments are confirmed by the coupling constants of the lactone. These suggest that the conformation of the lactone deviates significantly from that of a chair. The –5.6 Hz geminal coupling between H(18) and C(71.87) is indicative of a *gauche* relationship between H(18) and the lactone oxygen atom, whereas the –1.2 Hz geminal coupling between H(8) and C(71.87) is indicative of an antiperiplanar relationship between H(8) and the lactone oxygen atom. This gives the correct structure of salvinorin A (which has been confirmed by total synthesis and single-crystal X-ray analysis).[73,75]

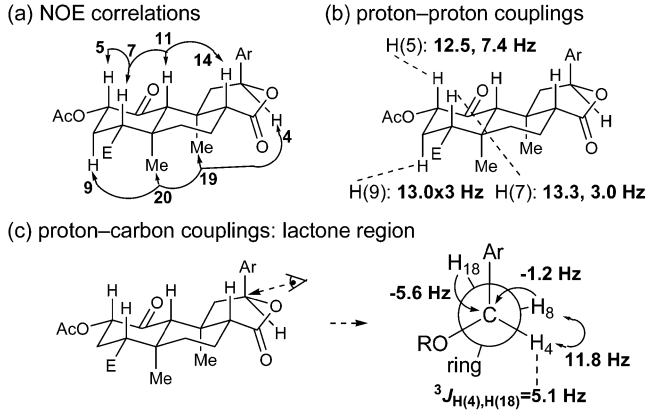

Figure 15. Relative stereochemistry of salvinorin A.

6. Experimental Considerations

6.1. Acquisition Parameters

The choice of appropriate acquisition parameters can significantly affect spectral quality, particularly for dilute samples. Two key parameters for 2D experiments are the number of increments (ni) and the delay between scans. Both the resolution in the indirectly detected dimension (e.g., ^{13}C for HSQC) and experimental time are proportional to *ni* (resolution in the directly detected dimension is proportional to acquisition time, and is usually not limiting). In most cases, both the default *ni* and delay time are too large (causing insufficient resolution, as discussed above for hexacyclinol, and signal lost, respectively).[14a] Table 1 lists recommended parameters for different concentrations and molecular weights. In general, more complex and larger molecules require more increments and shorter delays between scans.

The experiments described above are best performed with proton-optimized, or "inverse-detection" probes. Some experiments (Table 1) require the calibration of 90° pulse widths (^1H or ^{13}C) and tuning of the probe immediately before acquisition. This yields particular benefits for the HSQC experiment. These simple calibrations can be performed quickly (see Supporting Information). It should be noted that, for the HSQC experiment, samples are heated by decoupling during acquisition; therefore, the fraction of time during each scan spent on acquisition should be limited to 20% to avoid decomposition (10% for high dielectric solvents such as $[D_6]$DMSO).[11c] The use of variable-temperature regulation, even at room temperature, also helps mitigate this effect.

6.2. Processing Strategies

The manner in which 2D NMR spectroscopic datasets are processed can greatly influence spectral quality.[11c,14a] In general, "processing" refers to the conversion of raw datasets that contain two time axes to datasets that contain two chemical shift axes. By convention, these axes are referred to as F1 and F2, for the indirectly and directly detected dimensions, respectively (e.g., ^{13}C and ^1H for HSQC). Typically, the raw data are multiplied by apodization functions in both dimensions before performing a 2D Fourier transform (FT) (apodization increases signal to noise at the expense of resolution). Most software now contain an interactive mode in which the data before and after apodization can be compared; the weight of the apodization function should be adjusted to allow the FID to decay smoothly. Another procedure that can be simultaneously used to increase signal to noise by an additional factor of 2 to 4 is F1 linear prediction (LP).[77] Also available in many processing programs, this technique uses a mathematical algorithm to extend the dataset in F1 beyond what was actually collected.

Here is a specific example: Table 1 suggests "phase sensitive; 4 × LP in F1; Gaussian" as suitable processing parameters for a typical HSQC experiment. For a dataset containing 128 and 512 points in F1 and F2, respectively, this should be interpreted as "extend the data in F1 to 4 × 128 = 512 points by using linear prediction to predict points 257 to 512; then multiply the data in F1 and F2 by a Gaussian

apodization function; and finally, perform a 1024 × 1024 2D FT." In general, the use of eight coefficients for linear prediction is sufficient. The size of the FT should be at least twice the size of the largest number of points collected for optimum resolution. The term "phase-sensitive" indicates that peaks in the spectrum will appear either up or down. Phase-sensitive 2D spectra often require a minor phase adjustment, similar to that for 1D spectra. With modern computers, processing typically requires about five minutes.

6.3. Dilute Samples

The analysis of dilute solutions (1–5 mM) often requires the use of strategies that either increase concentration or enhance the sensitivity (Table 1). Commercially available low-volume NMR tubes that contain glass inserts with solvent-matched magnetic susceptibilities above and below the sample region can increase signal to noise by a factor of two, but are accompanied by moderate difficulties in shimming and concentration-related spectral changes. The use of micro- or cryoprobes can also allow the use of smaller sample containers and increase signal to noise significantly.

In recent years, gradient-selected versions of 2D NMR experiments have largely replaced their phase-cycled counterparts because they eliminate many of the "t_1 ridges" associated with intense signals. However, gradient-selected experiments are inherently 40% less sensitive than phase-cycled ones. Because random noise, not t_1 ridges, is the primary source of artifacts in dilute solutions, phase-cycled HSQC and HMBC spectra actually give superior signal-to-noise ratio (for various technical reasons, this advantage is less pronounced for other experiments).[78] Modest sensitivity gains can also be obtained by observing HSQC spectra without the spin-echo option, a modification that results in a uniform phase for all signals. Although typically acquired in absolute-value mode, sensitivity gains of approximately 40% and increased carbon resolution can be obtained by acquiring phase-cycled HMBC spectra in phase-sensitive mode.[79] These spectra are processed in "mixed mode": phase sensitive along the carbon axis and absolute value along the proton axis. Together, these measures make the analysis of 1–5 μmol possible within 12 to 24 h with a standard 5 mm inverse-detection probe.

7. Outlook and Conclusion

Although the use of through-bond correlation maps to establish structural connectivity is likely to remain standard procedure, newer technologies may soon supplement the use of the NOE and coupling constants for the determination of relative configuration. In particular, the use of residual dipolar couplings (RDCs) has great potential.[80] RDCs arise when the magnetic flux from one nucleus affects the magnetic field at another. This interaction is manifested as a coupling of size $J + D$, where J is the original coupling between the nuclei and D is the RDC. Although D depends strongly on both distance and orientation relative to the external magnetic field, averaging due to tumbling ordinarily reduces it to zero. To access RDCs, partially anisotropic media, such as liquid crystals or polymer gels, must be used.

Theoretically, a major advantage of RDCs is their longer range distance dependence (r^{-3}) compared to that of the NOE (r^{-6}). This may allow detailed stereochemical information to be derived from molecules for which NOE correlations are ambiguous or absent. However, both the interpretation of RDCs and the handling of samples in partially aligned media remain important challenges for this active area of research.

While new spectroscopic methods are continually emerging, developments in the computerized analysis of NMR spectroscopic data have been no less impressive.[81] Programs for dereplication,[82] the process of eliminating known compounds from groups of unknowns, are now widely available and can reliably help chemists avoid elucidating a compound twice. Additionally, predictions of chemical shifts and multiplet patterns are now quite useful, thanks to the availability of large empirical databases. In fact, the ultimate goal of reliable automated structure determination is now well within reach.[83] At a minimum, such programs can already assist users by proposing structures that might otherwise not have been considered. In some cases, computer programs have even been the primary analysis method used to deduce the structure of natural products.[84]

This Microreview has presented practical strategies for the spectroscopic elucidation of small organic molecules. The process of first determining skeletal connectivity and then relative configuration using through-bond correlation maps, NOE correlations, and coupling constants has proven to be robust and reliable. We hope that the discussions and detailed procedures provided herein will serve as a useful reference for organic chemists engaged in a wide range of structural elucidation tasks.

Supporting Information (see footnote on the first page of this article)**:** Detailed experimental procedures and sample spectra for menthol (interested readers are invited to reproduce these experiments before tackling their own unknowns), comparison of COSY-90 and COSY-45, comparison of CIGAR and HMBC, procedures for measuring $^1J_{C,H}$ with 1D-TOCSY, and spectra of salvinorin A.

Acknowledgments

E. E. K. thanks his advisor, Professor D. A. Evans, for his continuing support, Professor W. F. Reynolds for many helpful discussions, and the Natural Sciences and Engineering Research Council of Canada (NSERC) for a Julie Payette graduate fellowship. Mr. G. Maloney is warmly acknowledged for his editorial assistance.

[1] G. E. Martin, R. C. Crouch, *J. Nat. Prod.* **1991**, *54*, 1–70.
[2] W. F. Reynolds, R. G. Enríquez, L. I. Escobar, X. Lozoya, *Can. J. Chem.* **1984**, *62*, 2421–2425.
[3] M. F. Summers, L. G. Marzilli, A. Bax, *J. Am. Chem. Soc.* **1986**, *108*, 4285.
[4] S. B. Singh, H. Jayasuriya, J. G. Ondeyka, K. B. Herath, C. Zhang, D. L. Zink, N. N. Tsou, R. G. Ball, A. Basilio, O. Gen-

illoud, M. T. Diez, F. Vicente, F. Pelaez, K. Young, J. Wang, *J. Am. Chem. Soc.* **2006**, *128*, 11916–11920.
[5] S.-H. Li, J. Wang, X.-M. Niu, Y.-H. Shen, H.-J. Zhang, H.-D. Sun, M.-L. Li, Q.-E Tian, Y. Lu, P. Cao, Q.-T. Zheng, *Org. Lett.* **2004**, *6*, 4327–4330.
[6] S. J. Duncan, *J. Am. Chem. Soc.* **2001**, *123*, 554–560.
[7] C.-S. Li, Y.-T. Di, H.-P. He, S. Gao, Y.-H. Wang, Y. Lu, J.-L. Zhong, X.-J. Hao, *Org. Lett.* **2007**, *9*, 2509–2512.
[8] H. Jayasuriya, Z. Guan, J. D. Polishook, A. W. Dombrowski, P. J. Felock, D. J. Hazuda, S. B. Singh, *J. Nat. Prod.* **2003**, *66*, 551–553.
[9] T. Müller, D. Margraf, Y. Syha, *J. Am. Chem. Soc.* **2005**, *127*, 10852–10860.
[10] I. D'Acquarica, L. Nevola, G. D. Monache, E. Gács-Baitz, C. Massera, F. Ugozzoli, G. Zappia, B. Botta, *Eur. J. Org. Chem.* **2006**, 3652–3660.
[11] a) R. M. Silverstein, F.X. Webster in *Spectrometeric Identification of Organic Compounds*, 6th ed., John Wiley & Sons, Inc., **1998**; b) J. B. Lambert, H. F. Shurvell, D. A. Lightner, R.G. Cooks in *Organic Structural Spectroscopy*, Prentice-Hall, Inc., Upper Saddle River, New Jersey, **2001**; c) J. B. Lambert, E. P. Mazzola in *Nuclear Magnetic Resonance Spectroscopy: An Introduction to Principles, Applications, and Experimental Methods*, Inc. Pearson Education Upper Saddle River, New Jersey, **2004**.
[12] J. D. Roberts in *ABCs of FTNMR,* University Science Books, Sausalito, **2000**, p. 232.
[13] D. Neuhaus, M. P. Williamson in *The Nuclear Overhauser Effect in Structural and Conformational Analysis*, 2nd ed., Wiley-VCH, New York, **2000**, p. 37.
[14] Recent reviews: a) W. F. Reynolds, R. G. Enríquez, *J. Nat. Prod.* **2002**, *65*, 221–244; b) E. Fukushi, *Biosci. Biotechnol. Biochem.* **2006**, *70*, 1803–1812; c) N. Bross-Walch, T. Kühn, D. Moskau, O. Zerbe, *Chem. Biodiv.* **2005**, *2*, 147–177.
[15] Because overlapping peaks are a prominent cause of difficult analyses, it is often worth experimenting with solvents other than $CDCl_3$. A particularly useful procedure is to add [D_6]benzene dropwise to a sample dissolved in $CDCl_3$/C_6D_6 (10:1, or vice versa) while monitoring the spectrum between drops. This often gives an acceptable spectrum even when the spectra in pure $CDCl_3$ and C_6D_6 are unclear. Even if no one solvent mixture completely separates every peak, information can be combined from two solvent mixtures to give a complete picture. The replacement of $CDCl_3$ by CD_2Cl_2 should also be considered, because $CDCl_3$ can produce protic acid in the presence of light and oxygen via phosgene. Also see ref.[2]
[16] M. Badertscher, K. Bischofberger, M. E. Munk, E. Pretsch, *J. Chem. Inf. Comput. Sci.* **2001**, *41*, 889–893.
[17] Original report: G. Bodenhausen, D. J. Ruben, *Chem. Phys. Lett.* **1980**, *69*, 185–189.
[18] By convention, CH_3, CH_2, CH, and C fragments are respectively referred to as methyl, methylene, methine, and quaternary carbon atoms in the context of NMR spectroscopy, regardless of what other groups are attached.
[19] J. N. Shoolery, S. Patts, *J. Magn. Reson.* **1982**, *46*, 535–539.
[20] a) M. R. Bendall, D. M. Dodrell, D. T. Pegg, *J. Am. Chem. Soc.* **1981**, *103*, 4603–4605; b) G. A. Morris, R. Freeman, *J. Am. Chem. Soc.* **1979**, *101*, 760–762.
[21] A. Bax, S. Subramanian, *J. Magn. Reson.* **1986**, *67*, 565–569.
[22] A. Bax, *J. Magn. Reson.* **1983**, *53*, 517–520.
[23] P. E. Hansen, *Prog. Nucl. Magn. Reson. Spect.* **1981**, *14*, 175–296.
[24] Detailed discussions can be found in refs.[11c,14a]
[25] T. R. Hoye, H. Zhao, *J. Org. Chem.* **2002**, *67*, 4014–4016.
[26] A. Bax, R. Freeman, *J. Magn. Reson.* **1981**, *44*, 542–561.
[27] W. E. Hull in *Two Dimensional NMR Spectroscopy: Applications for Chemists and Biochemists*, 2nd ed. (Eds: W. R. Croasmun, R. M. K. Carlson,), VCH, New York, **1994**, p. 302.
[28] This is because of the differing levels of resolution in F2 (high, shows small couplings) and F1 (low, may not show small couplings). Symmetrization removes this effect, and in addition, can create false cross peaks. With modern spectrometer hardware, it is unnecessary and its use is not recommended.
[29] T. Fäcke, S. Berger, *J. Magn. Reson. Ser. A* **1995**, *113*, 257–259.
[30] Exceptions are possible: J. Cavanagh, W. J. Zhazin, M. Rance, *J. Magn. Reson.* **1990**, *87*, 110–131.
[31] A. Bax, M. F. Summers, *J. Am. Chem. Soc.* **1986**, *108*, 2093–2094.
[32] R. Araya-Maturana, T. Delgado-Castro, W. Cardona, B. E. Weiss-López, *Curr. Org. Chem.* **2001**, *5*, 253–263.
[33] a) C. E. Hadden, G. E. Martin, V. V. Krishnamurthy, *Magn. Reson. Chem.* **2000**, *38*, 143–147; b) G. E. Martin, C. E. Hadden, R. C. Crouch, V. V. Krishnamurthy, *Magn. Reson. Chem.* **1999**, *37*, 517–528.
[34] An extensive review: G. E. Martin, C. E. Hadden, *J. Nat. Prod.* **2000**, *63*, 543–585.
[35] D. H. Williams, *Acc. Chem. Res.* **1984**, *17*, 364–369 (and refs. therein).
[36] J. M. Seco, E. Quiñoá, R. Riguera, *Chem. Rev.* **2004**, *104*, 17–117.
[37] K. Stott, J. Keeler, Q. N. Van, A. J. Shaka, *J. Magn. Reson.* **1997**, *125*, 302–304.
[38] T. D. W. Claridge in *Tetrahedron Organic Chemistry Series Vol. 19: High-Resolution NMR Techniques in Organic Chemistry* (Eds.: J. E. Baldwin, R. M. Williams), Elsevier, Oxford, **1999**, pp. 117–118.
[39] a) T.-L. Hwang, A. J. Shaka, *J. Am. Chem. Soc.* **1992**, *114*, 3157–3159; b) W. Bauer, A. Soi, A. Hirsch, *Magn. Reson. Chem.* **2000**, *38*, 500–503; c) A. A. Bothner-By, R. L. Stephens, J.-M. Lee, C. D. Warren, R. W. Jeanloz, *J. Am. Chem. Soc.* **1996**, *118*, 811–813.
[40] S. Macura, Y. Huang, D. Suter, R. R. Ernst, *J. Magn. Reson.* **1981**, *43*, 259–281.
[41] M. Eberstadt, G. Gemmecker, D. F. Mierke, H. Kessler, *Angew. Chem. Int. Ed. Engl.* **1995**, *34*, 1671–1695.
[42] M. Karplus, *J. Am. Chem. Soc.* **1963**, *85*, 2870–2871.
[43] S. J. Duncan, R. Lewis, M. A. Bernstein, P. Sandor, *Magn. Reson. Chem.* **2007**, *45*, 283–288.
[44] Ref. [38], pp.117–118.
[45] a) V. Piantini, O. W. Sorensen, R. R. Ernst, *J. Am. Chem. Soc.* **1982**, *104*, 6800–6801; b) M. Rance, G. Sørensen, G. Bodenhausen, G. Wagner, R. R. Ernst, K. Wüthrich, *Biochem. Biophys. Res. Commun.* **1983**, *117*, 479–485.
[46] C. Griesinger, O. W. Sorensen, R. R. Ernst, *J. Am. Chem. Soc.* **1985**, *107*, 6394–6396.
[47] a) Ref.[41], p. 1681; b) ref.[38], pp. 192–196; c) ref.[14a], p. 226.
[48] Calculations carried out with WinDNMR: H. J. Reich, *J. Chem. Educ. Software*, **1996**, 3D2.
[49] Ref. [12], pg. 233.
[50] A. S. Perlin, B. Casu, *Tetrahedron Lett.* **1969**, *10*, 2921–2924.
[51] B. L. Marquez, W. H. Gerwick, R. T. Williamson, *Magn. Reson. Chem.* **2001**, *39*, 499–530.
[52] a) N. Matsumori, D. Kaneno, M. Murata, H. Nakamura, K. Tachibana, *J. Org. Chem.* **1999**, *64*, 866–876; b) G. Bifulco, P. Dambruso, L. Gomez-Paloma, R. Riccio, *Chem. Rev.* DOI: 10.1021/cr030733c.
[53] M. Karplus, *J. Am. Chem. Soc.* **1962**, *84*, 2870–2871.
[54] M. Karplus, *J. Am. Chem. Soc.* **1962**, *84*, 2458–2460.
[55] N. Matsumori, M. Murata, K. Tachibana, *Tetrahedron* **1995**, *51*, 12229–12238.
[56] D. Uhrín, G. Batta, V. J. Hruby, P. N. Barlow, K. E. Kövér, *J. Magn. Reson.* **1998**, *130*, 155–161.
[57] P. Vidal, N. Esturau, T. Parella, J. F. Espinosa, *J. Org. Chem.* **2007**, *72*, 3166–3170.
[58] J. Li, S. Jeong, L. Esser, P. G. Harran, *Angew. Chem. Int. Ed.* **2001**, *40*, 4765–4769.
[59] B. Schlegel, A. Härtl, H.-M. Dahse, F. A. Gollmick, U. Gräfe, H. Dörfelt, B. Kappes, *J. Antibiot.* **2002**, *55*, 814–817.
[60] S. D. Rychnovsky, *Org. Lett.* **2006**, *8*, 2895.

[61] J. A. Porco Jr, S. Su, X. Lei, S. Bardhan, D. Rychnovsky, *Angew. Chem. Int. Ed.* **2006**, *45*, 5790–5792.
[62] See ref.[61], Supporting Information, p. 9.
[63] W. F. Professor Reynolds, University of Toronto, personal communication.
[64] S. S. Golotvin, E. Vodopianov, R. Pol, B. A. Lefebvre, A. J. Williams, R. D. Rutkowske, T. D. Spitzer, *Magn. Reson. Chem.* **2007**, *45*, 803–813.
[65] J. B. Lowry, N. V. Riggs, *Tetrahedron Lett.* **1964**, *5*, 2911–2917.
[66] M. Köck, A. Grube, I. B. Seiple, P. S. Baran, *Angew. Chem. Int. Ed.* **2007**, *46*, 6586–6594.
[67] P. Sharma, M. Alam, *J. Chem. Soc. Perkin Trans. 1* **1988**, 2537–2540.
[68] a) L. A. Paquette, O. M. Moradei, P. Bernardelli, T. Lange, *Org. Lett.* **2000**, *2*, 1875–1878; b) L. E. Overman, L. D. Pennington, *Org. Lett.* **2000**, *2*, 2683–2686.
[69] D. Friedrich, R. W. Doskotch, L. A. Paquette, *Org. Lett.* **2000**, *2*, 1879–1882.
[70] F. Gallou, D. W. C. MacMillan, L. E. Overman, L. A. Paquette, L. D. Pennington, J. Yang, *Org. Lett.* **2001**, *3*, 135–137.
[71] S. M. Weinreb, *Acc. Chem. Res.* **2003**, *36*, 59–65.
[72] K. Justus, R. Herrmann, J.-D. Klamann, G. Gruber, V. Hellwig, A. Ingerl, K. Polborn, B. Steffan, W. Steglich, *Eur. J. Org. Chem.* **2007**, *33*, 5560–5572.
[73] A. Ortega, J. F. Blount, P. S. Manchand, *J. Chem. Soc. Perkin Trans. 1* **1982**, *10*, 2505–2508.
[74] T. A. Munro, M. A. Rizzacasa, B. L. Roth, B. A. Toth, F. Yan, *J. Med. Chem.* **2005**, *48*, 345–348.
[75] J. R. Scheerer, J. F. Lawrence, G. C. Wang, D. A. Evans, *J. Am. Chem. Soc.* **2007**, *129*, 8968–8969.
[76] a) The chemical shifts and solvent mixture were taken from: J.-L. Giner, D. J. Kiemle, L. Kutrzeba, J. Zjawiony, *Magn. Reson. Chem.* **2007**, *45*, 351–354. 2D NMR correlations were obtained by the authors (500 MHz, inverse-detected probe). For clarity, weak four- and five-bond HMBC correlations have been omitted. b) Proton–carbon coupling constants were measured by HETLOC (20 ms mixing time).
[77] W. F. Reynolds, M. Yu, R. G. Enriquez, *Magn. Reson. Chem.* **1997**, *35*, 505–519.
[78] W. F. Reynolds, R. G. Enríquez, *Magn. Reson. Chem.* **2001**, *39*, 531–538.
[79] A. Bax, D. Marion, *J. Magn. Reson.* **1988**, *78*, 186–191.
[80] a) R. M. Gschwind, *Angew. Chem. Int. Ed.* **2005**, *44*, 4666–4668; b) C. M. Thiele, *Concepts Magn. Res. Part A* **2007**, *30*, 65–80.
[81] C. Steinbeck, *Nat. Prod. Rep.* **2004**, *21*, 512–518.
[82] R. T. Williamson, E. L. Chapin, A. W. Carr, J. R. Gilbert, P. R. Graupner, P. Lewer, P. McKamey, J. R. Carney, W. H. Gerwick, *Org. Lett.* **2000**, *2*, 289–292.
[83] a) Y. D. Smurnyy, M. E. Elyashberg, K. Blinov, B. A. Lefebvre, G. E. Martin, A. J. Williams, *Tetrahedron* **2005**, *61*, 9980–9989; b) R. Dunkel, X. Wu, *J. Magn. Reson.* **2007**, *188*, 97–110.
[84] K. Blinov, M. Elyashberg, E. R. Martirosian, S. G. Molodtsov, A. J. Williams, A. N. Tackie, M. M. H. Sharaf, P. L. Schiff Jr, R. C. Crouch, G. E. Martin, C. E. Hadden, J. E. Guido, K. A. Mills, *Magn. Reson. Chem.* **2003**, *41*, 577–584.

Received: October 12, 2007
Published Online: March 25, 2008

